Optical Modes of Vibration in an Ionic Crystal Slab Including Retardation. I. Nonradiative Region*

K. L. KLIEWER AND RONALD FUCHS
Institute for Atomic Research and Department of Physics, Iowa State University, Ames, Iowa
(Received 12 November 1965)

The optical modes of vibration in an ionic crystal of finite thickness are found for wavelengths long compared to the interionic spacing. Retardation of the Coulomb interaction between the ions is included by solving the complete set of Maxwell's equations for the electromagnetic fields. Only the nonradiative modes, which have exponentially decreasing fields outside the slab, are discussed. The theoretical dispersion curves for various classes of modes in selected thicknesses of LiF are shown and are compared with the dispersion curves occurring without retardation.

I. INTRODUCTION

IN a previous paper[1] we determined the long-wavelength optical-mode frequencies for an ionic crystal slab, neglecting the effects due to the retardation of the Coulomb interaction. The frequencies were determined as a function of the wave-vector component k_x parallel to the slab (Fig. 1), rather than the three-dimensional wave vector $\mathbf{k}$ as in the case of an infinite crystal. We found that the longitudinal modes are all at ω_L, the usual $k\sim 0$ longitudinal optical (LO) frequency in an infinite crystal, and that a series of transverse modes are at ω_T, the usual transverse optical (TO) frequency. In addition there are two optical branches having exponential z dependence inside the slab. The frequencies of these "surface" modes are at ω_T and ω_L for $k_x=0$, move together as k_x increases, and approach a frequency between ω_T and ω_L when $k_x \gg \omega_T/c$.

We have now extended the calculation to take account of retardation. The dispersion relation for long-wavelength phonons in an infinite crystal, when retardation is included, no longer consists of two parallel straight lines ($\omega=\omega_L$, $\omega=\omega_T$), but is given by the expression $k^2=\epsilon\omega^2/c^2$, where $\epsilon(\omega)$ is the frequency-dependent dielectric constant.[2] This dispersion relation describes the coupled phonon-photon system instead of simply the phonon system alone. A similar coupling between phonons and photons and a corresponding alteration of the dispersion relation occurs in a slab. The finite thickness of the slab, however, causes the modes to fall into two classes: (1) nonradiative modes with exponentially damped fields outside the slab, and (2) radiative modes, with incoming or outgoing waves outside the slab. In this paper we restrict ourselves to the nonradiative modes, which, in the case of a crystal with no intrinsic damping (ϵ real), are true normal modes in the sense that they persist forever after being initially excited. The radiative modes are not true normal modes since they are highly damped even when ϵ is real. A discussion of the radiative modes and their relation to the optical properties of the slab will be published in the future.

In the following section we derive the dispersion relations for the nonradiative modes in the wavelength region $\lambda \gg r_0$, where r_0 is the interionic spacing. The treatment is similar to that of Sec. III in Ref. 1. By using Maxwell's equations written in terms of macroscopic fields and polarization, the local electric field at a given ion can be expressed as an integral over the polarization at distant regions of the crystal. By writing the equations of motion for the ions in terms of these expressions for the local fields, integral equations for the polarization are derived. The frequency-dependent dielectric constant emerges at the end of the derivation.

In the Appendix we present an alternative derivation of the dispersion relations. In this method, we initially relate the field at a given point to the polarization at the same point by the dielectric constant; there is no longer an integral over the polarization at distant points. The problem reduces to a very simple application of Maxwell's equations with the usual boundary conditions at the surface of the slab. The equivalence of these methods is closely related to the Ewald-Oseen extinction theorem,[3] which states that if one superposes the radiation fields of induced dipoles in a dielectric and the field of a primary plane wave, where all fields propagate with the velocity c, the primary wave is cancelled exactly by part of the dipole fields and the resultant field is a plane wave propagating with the velocity $c/\sqrt{\epsilon}$.

II. NORMAL MODES

In this section we investigate the optical modes of vibration of the ionic crystal slab sketched in Fig. 1 for wavelengths large compared to the interionic spacing. The inclusion of retardation requires a solution of the full set of Maxwell's equations which we write here as

$$\begin{aligned}
&\nabla\cdot\mathbf{E}=-4\pi\nabla\cdot\mathbf{P},\\
&\nabla\cdot\mathbf{B}=0,\\
&\nabla\times\mathbf{E}=-(1/c)(\partial\mathbf{B}/\partial t),\\
&\nabla\times\mathbf{B}=(1/c)(\partial\mathbf{E}/\partial t)+(4\pi/c)(\partial\mathbf{P}/\partial t),
\end{aligned}\tag{2.1}$$

* Work was performed at the Ames Laboratory of the U. S. Atomic Energy Commission. Contribution No. 1823.

[1] R. Fuchs and K. L. Kliewer, Phys. Rev. 140, A2076 (1965).

[2] M. Born and K. Huang, *Dynamical Theory of Crystal Lattices* (Oxford University Press, London, 1954), Chap. II, Sec. 8.

[3] M. Born and E. Wolf, *Principles of Optics* (Pergamon Press, New York, 1964), 2nd ed., Sec. 2.4.

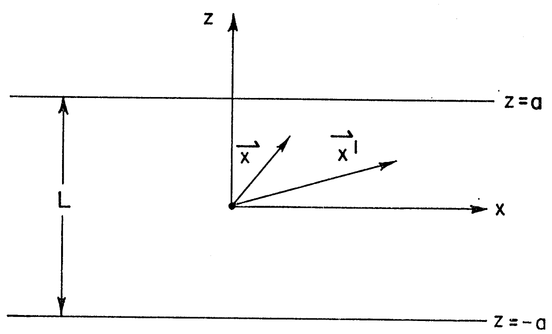

FIG. 1. Diagram of the coordinate system and various parameters used in discussing the ionic crystal slab.

where $\mathbf{E}$ and $\mathbf{B}$ are macroscopic fields and $\mathbf{P}$ is the polarization. The charge density ρ and the current density $\mathbf{J}$ are clearly given by

$$\rho = -\nabla\cdot\mathbf{P}, \tag{2.2}$$

and

$$\mathbf{J} = (\partial\mathbf{P}/\partial t). \tag{2.3}$$

We shall in this section carry out the calculation via the determination of the potentials $\mathbf{A}$ and Φ as ordinarily defined.

Working in the Coulomb gauge where $\nabla\cdot\mathbf{A}=0$, the equations determining the potentials are

$$\Phi(\mathbf{x},t) = -\int \frac{\nabla\cdot\mathbf{P}(\mathbf{x}',t)}{|\mathbf{x}-\mathbf{x}'|} d^3x', \tag{2.4}$$

and

$$\nabla^2\mathbf{A} - \frac{1}{c^2}\frac{\partial^2\mathbf{A}}{\partial t^2} = \frac{1}{c}\nabla\left(\frac{\partial\Phi}{\partial t}\right) - \frac{4\pi}{c}\frac{\partial\mathbf{P}}{\partial t}. \tag{2.5}$$

Orienting the crystal such that the component of the wave vector in the y direction is zero, we write $\mathbf{P}(\mathbf{x},t)$ and $\Phi(\mathbf{x},t)$ as

$$\mathbf{P}(\mathbf{x},t) = \mathbf{P}(z)e^{ik_x x}e^{-i\omega t}, \tag{2.6}$$

$$\Phi(\mathbf{x},t) = \Phi(\mathbf{x})e^{-i\omega t}. \tag{2.7}$$

The determination of the contributions to the electric field from the scalar potential in the Coulomb gauge when retardation is included is equivalent to the calculation of the electric field without retardation. The latter has been carried out in detail in Ref. 1, so the calculation will only be sketched here.

Using Eq. (2.4) the contribution of the bulk of the crystal to the potential is

$$\Phi(\mathbf{x})|_B = -e^{ik_x x}\int \frac{[ik_x P_x(z') + dP_z(z')/dz']e^{ik_x(x'-x)}d^3x'}{[(x-x')^2+(y-y')^2+(z-z')^2]^{1/2}}. \tag{2.8}$$

Since the derivatives concern us here we need to evaluate, for example,

$$\left.\frac{\partial\Phi(\mathbf{x})}{\partial x}\right|_B = e^{ik_x x}\int \frac{[ik_x P_x(z') + dP_z(z')/dz'](x-x')e^{ik_x(x'-x)}d^3x'}{[(x-x')^2+(y-y')^2+(z-z')^2]^{3/2}}, \tag{2.9}$$

which is equal to

$$\left.\frac{\partial\Phi(\mathbf{x})}{\partial x}\right|_B = -2\pi i e^{ik_x x}\int_{-a}^{a} e^{-k_x|z-z'|}\left[ik_x P_x(z') + \frac{dP_z(z')}{dz'}\right]dz'. \tag{2.10}$$

After adding the surface polarization charge and integrating the bulk term by parts we find, inside the slab,

$$\left.\frac{\partial\Phi(\mathbf{x})}{\partial x}\right|_{\text{in}} = e^{ik_x x}\left[\int_{-a}^{a} G(z,z')P_x(z')dz' - i\int_{-a}^{a}\tilde{G}(z,z')P_z(z')dz'\right], \tag{2.11}$$

where

$$\begin{aligned} G(z,z') &= 2\pi k_x e^{-k_x|z-z'|}, \\ \tilde{G}(z,z') &= 2\pi k_x e^{-k_x(z'-z)}, \quad z'>z; \\ &= -2\pi k_x e^{-k_x(z-z')}, \quad z>z'. \end{aligned} \tag{2.12}$$

Similarly, we find

$$\left.\frac{\partial\Phi(\mathbf{x})}{\partial y}\right|_{\text{in}} = 0 \tag{2.13}$$

and

$$\left.\frac{\partial\Phi(\mathbf{x})}{\partial z}\right|_{\text{in}} = e^{ik_x x}\left[-\int_{-a}^{a} G(z,z')P_z(z')dz' - i\int_{-a}^{a}\tilde{G}(z,z')P_x(z')dz' + 4\pi P_z(z)\right], \tag{2.14}$$

the last term in Eq. (2.14) arising from the special treatment necessary for the region $z\simeq z'$.

In the present case the fields outside the slab are also of importance. [In the following equations, (2.15–2.28), when discussing the fields outside the slab, the upper sign or symbol is to be taken for $z>a$, the lower one for

$z<-a$.] The scalar potential contributions are

$$\left.\frac{\partial\Phi(\mathbf{x})}{\partial x}\right|_{\text{out}}=e^{ik_xx}\left[\int_{-a}^{a}G(z,z')P_x(z')dz'\mp i\int_{-a}^{a}\tilde{G}(z,z')P_z(z')dz'\right], \tag{2.15}$$

$$\left.\frac{\partial\Phi(\mathbf{x})}{\partial z}\right|_{\text{out}}=e^{ik_xx}\left[-\int_{-a}^{a}G(z,z')P_z(z')dz'\mp i\int_{-a}^{a}\tilde{G}(z,z')P_x(z')dz'\right], \tag{2.16}$$

and

$$\left.\frac{\partial\Phi(\mathbf{x})}{\partial y}\right|_{\text{out}}=0. \tag{2.17}$$

Let us now consider the vector potential. Writing

$$\mathbf{A}(\mathbf{x},t)=\mathbf{A}(z)e^{ik_xx}e^{-i\omega t}, \tag{2.18}$$

the equations for $A_x(z)$, from Eq. (2.5), are

$$\left(\frac{d^2}{dz^2}-\alpha_0{}^2\right)A_x(z)\,|_{\text{in}}=-\frac{i\omega}{c}\int_{-a}^{a}G(z,z')P_x(z')dz'-\frac{\omega}{c}\int_{-a}^{a}\tilde{G}(z,z')P_z(z')dz'+\frac{4\pi i\omega}{c}P_x(z), \tag{2.19}$$

and

$$\left(\frac{d^2}{dz^2}-\alpha_0{}^2\right)A_x(z)\Big|=-\frac{i\omega}{c}\int_{-a}^{a}G(z,z')P_x(z')dz'\mp\frac{\omega}{c}\int_{-a}^{a}\tilde{G}(z,z')P_z(z')dz', \tag{2.20}$$

where

$$\alpha_0\equiv+(k_x{}^2-\omega^2/c^2)^{1/2}. \tag{2.21}$$

The solutions of these equations are

$$A_x(z)\,|_{\text{in}}=C_7e^{-\alpha_0z}+C_8e^{\alpha_0z}-\frac{ic}{\omega}\int_{-a}^{a}G(z,z')P_x(z')dz'-\frac{c}{\omega}\int_{-a}^{a}\tilde{G}(z,z')P_z(z')dz'$$
$$+\frac{ic}{\omega}\int_{-a}^{a}G'(z,z')P_x(z')dz'+\frac{c}{\omega}\int_{-a}^{a}\tilde{G}'(z,z')P_z(z')dz', \tag{2.22}$$

$$A_x(z)\Big|_{\text{out}}=\begin{pmatrix}C_1\\C_9\end{pmatrix}e^{-\alpha_0z}+\begin{pmatrix}C_2\\C_{10}\end{pmatrix}e^{+\alpha_0z}-\frac{ic}{\omega}\int_{-a}^{a}G(z,z')P_x(z')dz'\mp\frac{c}{\omega}\int_{-a}^{a}\tilde{G}(z,z')P_z(z')dz', \tag{2.23}$$

where

$$\begin{aligned}G'(z,z')&=2\pi\alpha_0e^{-\alpha_0|z-z'|},\\ \tilde{G}'(z,z')&=2\pi k_xe^{-\alpha_0(z'-z)},\quad z'>z,\\ &=-2\pi k_xe^{-\alpha_0(z-z')},\quad z>z',\end{aligned} \tag{2.24}$$

and the C_i are integration constants. Proceeding as above, the expressions for $A_y(z)$ and $A_z(z)$ become

$$A_y(z)\,|_{\text{in}}=C_{15}e^{-\alpha_0z}+C_{16}e^{\alpha_0z}-i\frac{\omega}{c}\frac{1}{\alpha_0{}^2}\int_{-a}^{a}G'(z,z')P_y(z')dz', \tag{2.25}$$

$$A_y(z)\Big|_{\text{out}}=\begin{pmatrix}C_5\\C_{17}\end{pmatrix}e^{-\alpha_0z}+\begin{pmatrix}C_6\\C_{18}\end{pmatrix}e^{\alpha_0z}, \tag{2.26}$$

$$A_z(z)\,|_{\text{in}}=C_{14}e^{-\alpha_0z}+C_{13}e^{\alpha_0z}+\frac{ic}{\omega}\int_{-a}^{a}G(z,z')P_z(z')dz'-\frac{c}{\omega}\int_{-a}^{a}\tilde{G}(z,z')P_x(z')dz'$$
$$-i\frac{k_x{}^2}{\alpha_0{}^2}\frac{c}{\omega}\int_{-a}^{a}G'(z,z')P_z(z')dz'+\frac{c}{\omega}\int_{-a}^{a}\tilde{G}'(z,z')P_x(z')dz', \tag{2.27}$$

$$A_z(z)\Big|_{\text{out}}=\begin{pmatrix}C_3\\C_{11}\end{pmatrix}e^{-\alpha_0z}+\begin{pmatrix}C_4\\C_{12}\end{pmatrix}e^{\alpha_0z}+i\frac{c}{\omega}\int_{-a}^{a}G(z,z')P_z(z')dz'\mp\frac{c}{\omega}\int_{-a}^{a}\tilde{G}(z,z')P_x(z')dz'. \tag{2.28}$$

Having now equations for the potentials, it is a straightforward matter to obtain the fields. Applying the boundary conditions $\mathbf{B}$ continuous, E_x and E_y continuous, and $E_z+4\pi P_z$ continuous, at $z=\pm a$, gives 12 equations with 18 arbitrary constants. The requirement that $\nabla\cdot\mathbf{A}=0$ means, however, that $C_{11}=ik_xC_9/\alpha_0$, $C_{12}=-ik_xC_{10}/\alpha_0$, $C_3=ik_xC_1/\alpha_0$, $C_4=-ik_xC_2/\alpha_0$, $C_{14}=ik_xC_7/\alpha_0$, and $C_{13}=-ik_xC_8/\alpha_0$, so that we are left with 12 undetermined constants.

Because of the manner in which the crystal was oriented, the remaining equations split into two groups, six associated with the x-z directions and six associated with the y direction. We consider these two cases separately. In addition, since we are considering the nonradiative region in the present paper, α_0 is real or $|k_x|>\omega/c$.

x and z Directions

In order that the fields remain finite as $|z|\to\infty$, we must have $C_2=C_9=0$. This in turn means $C_7=C_8=0$ and

$$C_1=2\pi i\alpha_0\frac{c}{\omega}\int_{-a}^{a}e^{\alpha_0 z'}\left\{P_x(z')+\frac{ik_x}{\alpha_0}P_z(z')\right\}dz',$$

$$C_{10}=2\pi i\alpha_0\frac{c}{\omega}\int_{-a}^{a}e^{-\alpha_0 z'}\left\{P_x(z')-\frac{ik_x}{\alpha_0}P_z(z')\right\}dz',$$

so that the electric field components within the slab become (we write $\mathbf{E}(\mathbf{x},t)=\mathbf{E}(z)e^{ik_xx}e^{-i\omega t}$):

$$E_x(z)=-\int_{-a}^{a}G'(z,z')P_x(z')dz'+i\int_{-a}^{a}\tilde{G}'(z,z')P_z(z')dz', \quad (2.29)$$

and

$$E_z(z)=\int_{-a}^{a}G'(z,z')P_z(z')dz'+i\int_{-a}^{a}\tilde{G}'(z,z')P_x(z')dz'-4\pi P_z(z). \quad (2.30)$$

Defining $\mathbf{u}(\mathbf{x},t)$ *as* the relative displacement of the positive and negative ions,

$$\mathbf{u}(\mathbf{x},t)=\mathbf{u}_+(\mathbf{x},t)-\mathbf{u}_-(\mathbf{x},t),$$

the equation of motion within the slab is

$$\mu\partial^2\mathbf{u}(\mathbf{x},t)/\partial t^2=-\mu\omega_0^2\mathbf{u}(\mathbf{x},t)+e[\mathbf{E}(\mathbf{x},t)+4\pi\mathbf{P}(\mathbf{x},t)/3], \quad (2.31)$$

where μ is the reduced mass and ω_0 is the mechanical frequency arising from the short-range repulsive interaction. The term $4\pi\mathbf{P}/3$ is due to the local field correction. Assuming, for simplicity, that we are dealing with point ions ($\epsilon_\infty=1$),

$$\mathbf{u}(\mathbf{x},t)=\mathbf{P}(\mathbf{x},t)/ne, \quad (2.32)$$

where n is the density of ion pairs. Using Eqs. (2.6) and (2.29) through (2.32), the equations for the polarization are finally

$$R_xP_x(z)=-\int_{-a}^{a}G'(z,z')P_x(z')dz'+i\int_{-a}^{a}\tilde{G}'(z,z')P_z(z')dz', \quad (2.33)$$

and

$$R_zP_z(z)=\int_{-a}^{a}G'(z,z')P_z(z')dz'+i\int_{-a}^{a}\tilde{G}'(z,z')P_x(z')dz', \quad (2.34)$$

where

$$R_x=(\mu/ne^2)(\omega_0^2-\omega^2)-4\pi/3,$$
$$R_z=(\mu/ne^2)(\omega_0^2-\omega^2)+8\pi/3. \quad (2.35)$$

For R_x and R_z not equal to zero, we can obtain a differential equation for $P_x(z)$ by differentiating Eq. (2.33) twice and then replacing dP_z/dz by the derivative of Eq. (2.34). The result is

$$R_xd^2P_x/dz^2=[\alpha_0^2R_x+4\pi\alpha_0^2-4\pi k_x^2R_x/R_z-16\pi^2k_x^2/R_z], \quad (2.36)$$

which can be simplified to

$$d^2P_x/dz^2=[\alpha_0^2-4\pi\omega^2/R_xc^2]P_x. \quad (2.37)$$

The term in the brackets can be written, using Eq. (2.21), as

$$k_x^2-(\omega^2/c^2)(1+4\pi/R_x),$$

but $1+4\pi/R_x$ is just the expression for the dielectric constant without damping,

$$\epsilon=1+(4\pi ne^2/\mu)(\omega_0^2-\omega^2-4\pi ne^2/3\mu)^{-1}. \quad (2.38)$$

Note that the dielectric constant has not been inserted at any point, but has arisen naturally in the development. Defining

$$\alpha=+(k_x^2-\epsilon\omega^2/c^2)^{1/2}, \quad (2.39)$$

Eq. (2.37) becomes

$$d^2P_x(z)/dz^2=\alpha^2P_x(z) \quad (2.40)$$

and thus

$$P_x(z)=K_1e^{\alpha z}+K_2e^{-\alpha z}, \quad (2.41)$$

where K_1 and K_2 are integration constants. From Eqs. (2.33) and (2.34) we find, in addition,

$$P_z(z)=-\frac{ik_x}{\alpha^2}\frac{dP_x(z)}{dz}=-\frac{ik_x}{\alpha}(K_1e^{\alpha z}-K_2e^{-\alpha z}). \quad (2.42)$$

Using Eqs. (2.41) and (2.42) in the integral equations (2.33) and (2.34) yields terms which depend on z via $e^{\pm\alpha z}$ and $e^{\pm\alpha_0 z}$. The terms containing the factors $e^{\pm\alpha z}$ cancel, while equating the coefficients of the factors $e^{\pm\alpha_0 z}$ to zero individually gives a pair of homogeneous,

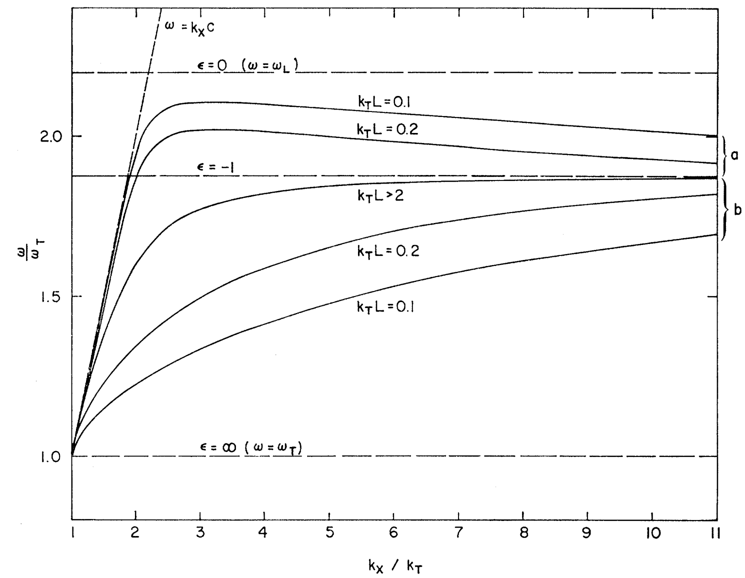

FIG. 2. The frequencies of transverse optical surface modes, as a function of k_x/k_T. The slab thickness is expressed as the dimensionless quantity $k_T L$. (a) High-frequency modes; (b) low-frequency modes.

linear equations in K_1 and K_2. The condition that there be a solution is

$$\epsilon = \frac{\alpha}{\alpha_0}\left(\frac{e^{-\alpha a} \mp e^{\alpha a}}{e^{-\alpha a} \pm e^{\alpha a}}\right). \tag{2.43}$$

Suppose α is real. Then the upper sign yields

$$\epsilon = -(\alpha/\alpha_0) \tanh \alpha a \tag{2.44}$$

and corresponds to $K_2 = -K_1$, so that

$$P_x(z) \propto \sinh \alpha z,$$
$$P_z(z) \propto -i(k_x/\alpha) \cosh \alpha z. \tag{2.45}$$

The lower sign in (2.43) corresponds to

$$\epsilon = -(\alpha/\alpha_0) \coth \alpha a, \tag{2.46}$$

with $K_1 = K_2$ and

$$P_x(z) \propto \cosh \alpha z,$$
$$P_z(z) \propto -i(k_x/\alpha) \sinh \alpha z. \tag{2.47}$$

The fact that α is real for these modes means that the frequencies lie between ω_T and ω_L, the ordinary $k \sim 0$ optical frequencies, where $\epsilon < 0$. In addition, these modes are localized at the surfaces for large values of αa, and thus we identify them as surface modes.

Equations (2.44) and (2.46) determine the surface mode frequencies as a function of k_x, and have been solved using parameters representing LiF. Atomic polarizabilities are included by replacing Eq. (2.38) by the expression

$$\epsilon = \epsilon_\infty + (\epsilon_0 - \epsilon_\infty)/(1 - \omega^2/\omega_T^2), \tag{2.48}$$

where $\epsilon_\infty = 1.92$, $\epsilon_0 = 9.27$, and $\omega_T = 5.78 \times 10^{13}$ sec^{-1}.[4] The solutions to Eqs. (2.44) and (2.46) are the high- and low-frequency surface modes, respectively, and are shown by the sets of curves labeled "a" and "b" in Fig. 2 for three values of the slab thickness $k_T L$, where $k_T = \omega_T/c$.

If $k_x \gg k_T$, $\omega/\omega_T \rightarrow 1.875$, a frequency corresponding to $\epsilon = -1$. The most significant effect of retardation occurs for small values of k_x. Without retardation the high- and low-frequency surface modes approach ω_L and ω_T as $k_x \rightarrow 0$, as shown in Fig. 2(b) of Ref. 1. When retardation is included, these modes exist only for $k_x > \omega/c$. In addition, ω for the high-frequency modes in thin crystals does not continue to increase with decreasing k_x, but decreases rapidly to ω_T as $k_x \rightarrow k_T$. Thus, the frequencies of both branches approach ω_T as $k_x \rightarrow k_T$. For thick crystals the low- and high-frequency modes fall along essentially the same curve, with ω a monotonically increasing function of k_x; in the case of the high-frequency modes, this is completely different from the monotonically decreasing behavior without retardation.

The spatial dependence and direction of polarization of the surface modes, as given by Eqs. (2.45) and (2.47), is also influenced by retardation. First suppose that retardation is neglected; then $\alpha = k_x$ in these equations. In a very thin slab ($k_x L \ll 1$), the polarization for the high-frequency mode is $P_x \propto \sinh k_x z \rightarrow 0$, $P_z \propto -i \cosh k_x z \rightarrow -i$; for the low-frequency mode, $P_x \propto \cosh k_x z \rightarrow 1$, $P_z \propto -i \sinh k_x z \rightarrow 0$. Thus the motion is roughly uniform across the slab if $k_x L \ll 1$ and is either normal or parallel to the slab.

Now suppose that retardation is included by restoring the original definition of α [Eq. (2.39)] in Eqs. (2.45) and (2.47). If the thin slab is characterized by the condition $k_T L \ll 1$, then there is a range of k_x for which $k_T L \ll \alpha L \ll 1$. If k_x is in this range, retardation affects only the frequencies of the normal modes; the solutions are ($P_x \sim 0$, $P_z \sim$ const) or ($P_x \sim$ const, $P_z \sim 0$), as they

[4] H. Bilz, L. Genzel, and H. Happ, Z. Physik **160**, 535 (1960).

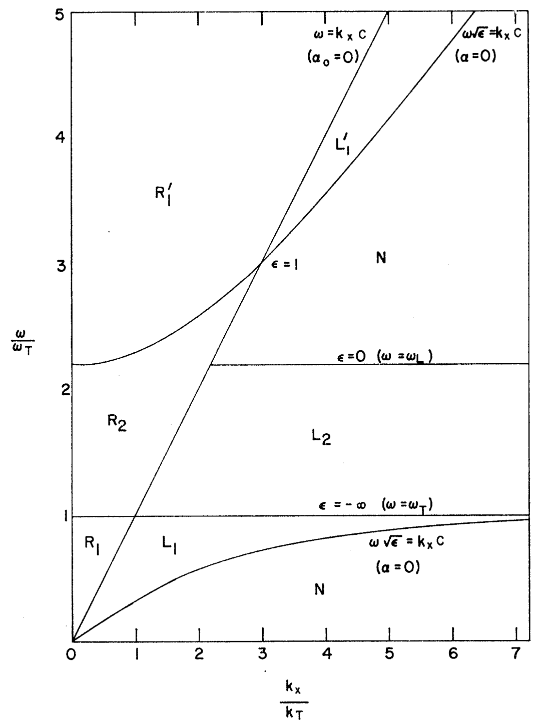

FIG. 3. Regions in the k_x,-ω plane for which different classes of transverse optical modes exist. The curves have been drawn for LiF, in which $\omega_T = 5.78 \times 10^{13}$ sec^{-1}, $k_T = \omega_T/c = 1.927 \times 10^3$ cm^{-1}, $\epsilon_0 = 9.27$, and $\epsilon_\infty = 1.92$. Radiative solutions exist in the regions R, and nonradiative (localized) solutions, in the regions L. The subscripts 1 and 2 denote, respectively, sinusoidal and real exponential solutions inside the slab. There are no solutions in the regions N.

are without retardation. However, when k_x approaches its lower limit k_T, then $\omega \rightarrow \omega_T$, $\epsilon \rightarrow -\infty$, and $\alpha \rightarrow \infty$. Thus αz becomes large, the polarization becomes localized at the surfaces, and $P_z \ll P_x$ for both the high- and low-frequency modes. In the limit $k_x \gg k_T$ the effects of retardation vanish; i.e., the magnitudes of P_x and P_z become equal, as they are without retardation.

The surface modes are transverse, in the sense that the polarization is solenoidal ($\nabla \cdot \mathbf{P} = 0$). It is, however, interesting that these transverse modes interact with conduction electrons as a consequence of both the finite size of the slab and the inclusion of retardation. First, consider the effect of the finite size. The electron-phonon interaction energy is proportional to $\int \mathbf{P} \cdot \mathbf{E}_{\text{vac}} d^3x$, where $\mathbf{E}_{\text{vac}}$ is the vacuum field of the condution electrons. If $\nabla \cdot \mathbf{P} = 0$, this volume integral vanishes only when the crystal is infinite; in a finite crystal the volume integral can be transformed into the nonvanishing surface integral $-\int \phi \mathbf{P} \cdot d\mathbf{s}$, where $\mathbf{E}_{\text{vac}} = -\nabla \phi$. In particular, this shows that electrons interact with the low-frequency surface mode in a thin slab, for which P_z predominates. In addition, retardation directly causes an electron-phonon interaction through the presence of the magnetic field.

The types of modes and the regions in the k_x—ω plane where they occur can be shown conveniently by drawing the curves $\omega = k_x c (\alpha_0 = 0)$ and $\omega\sqrt{\epsilon} = k_x c$ $(\alpha = 0)$, which define the boundaries of the regions (Fig. 3). The nonradiative regions, with fields approaching zero exponentially at infinity, are characterized by real α_0 or $k_x^2 > \omega^2/c^2$; they lie to the right of the line $\alpha_0 = 0$ and are labeled L_1, L_1', L_2, and N. The regions are further distinguished by the value of α. If α is real or $k_x^2 > \omega^2\epsilon/c^2$, there exist the "surface" modes which we have just discussed; these lie to the right of the curve $\alpha = 0$ in the regions N or L_2. Equations (2.44) and (2.46) imply that solutions exist only if $\epsilon < 0$ (region L_2); the regions marked N, for which $\epsilon > 0$, contain no solutions.

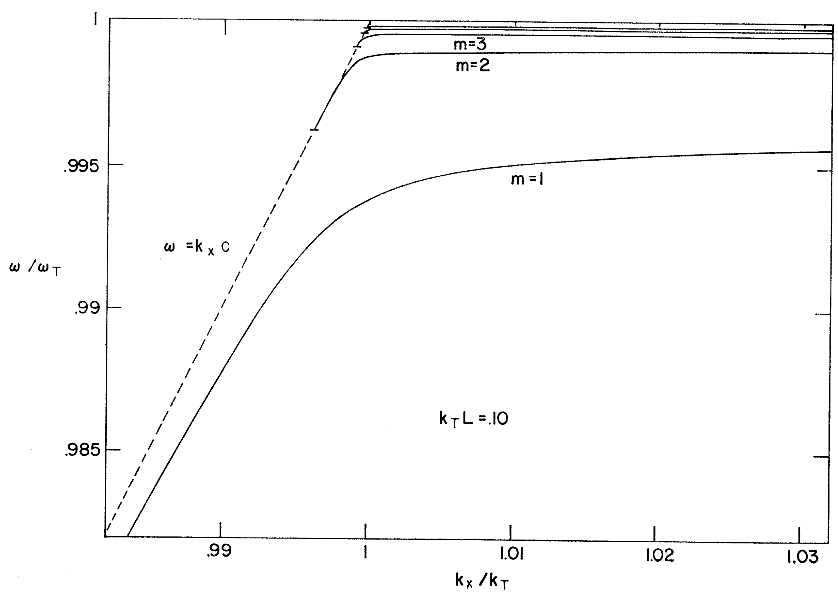

FIG. 4. Low-frequency, transverse, optical, xz-polarized modes for a thin slab with sinusoidal solutions inside the slab. Note that this graph shows only a very small portion of the k_x-ω plane near $\omega = \omega_T$ and $k_x = k_T$.

If, on the other hand, α is imaginary, the solutions inside the slab are oscillatory. The regions in Fig. 3 in which oscillatory solutions exist are designated by L_1 and L_1'. Thus, if we take $\alpha=i\beta$, the condition (2.44) that there be a solution becomes

$$\epsilon=(\beta/\alpha_0)\tan\beta a, \tag{2.49}$$

with

$$P_x(z)\propto i\sin\beta z,$$
$$P_z(z)\propto -(k_x/\beta)\cos\beta z, \tag{2.50}$$

and Eq. (2.46) becomes

$$\epsilon=-(\beta/\alpha_0)\cot\beta a, \tag{2.51}$$

with

$$P_x(z)\propto\cos\beta z,$$
$$P_z(z)\propto -i(k_x/\beta)\sin\beta z. \tag{2.52}$$

For LiF the solutions of Eqs. (2.49) and (2.51) which lie in region L_1 are shown for a thin slab in Fig. 4 and for a thick slab in Fig. 5, defining thin and thick with respect to the thickness corresponding to $k_TL=1$. These modes correspond to the TO modes which occur at ω_T without retardation; with retardation the frequencies lie below ω_T and depend on k_x.[5] More explicitly, without retardation the TO modes occur for $\beta=m\pi/L$, i.e., there is an integral number (m) of half-waves across the slab.[1] With retardation the modes can still be labeled by a positive integer m; however, $\beta<m\pi/L$, so that there is somewhat less than an integral number of half-waves across the slab because of the existence of exponentially decaying fields outside the slab. The modes with odd and even values of m are solutions of Eqs. (2.49) and (2.51), respectively. From Figs. 4 and 5 it can be seen that only the $m=1$ mode begins at $k_x=0$, $\omega=0$; the other modes begin at nonzero frequencies satisfying the equation $\beta L=(m-1)\pi$ on the line $\omega=k_xc$. If $k_x\gg k_T$, $\omega\longrightarrow\omega_T$ for all modes. For a thin slab (Fig. 4) the modes with $m>1$ are crowded closely near ω_T, but for a thick slab (Fig. 5) they extend over the entire frequency range below ω_T.

Equations (2.49) and (2.51) also have solutions in region L_1' (Fig. 6). The high-frequency sinusoidal modes exist only when retardation is included. The $m=1$ mode begins on the line $\omega=k_xc$ at the frequency $\omega=2.998\omega_T$ for which $\epsilon=1$, and the other modes begin at higher frequencies satisfying the equation $\beta L=(m-1)\pi$. The modes in a thin slab ($k_TL=0.1$) are difficult to show in a figure having the scale of Fig. 6, since the $m=1$ mode follows the line $\omega=k_xc$ very closely, and the $m=2$ mode begins at a relatively high frequency, $\omega=32.88\omega_T$. A thick slab, on the other hand, contains modes closely

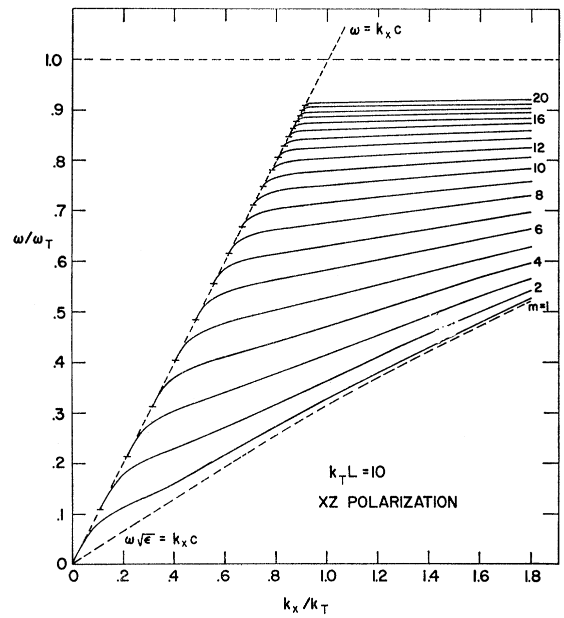

FIG. 5. Low-frequency, transverse, optical, xz-polarized modes for a thick slab with sinusoidal solutions inside the slab.

spaced in frequency. Both the low- and high-frequency sinusoidal modes in regions L_1 and L_1' can be considered as electromagnetic waves with an angle of incidence within the slab greater than the angle for total internal reflection, so that the waves are confined to the interior of the slab.

The complicated behavior of the sinusoidal modes in regions L_1 and L_1' is partly a consequence of the fact that ω is shown as a function of k_x. If we let k_c be the magnitude of the wave vector inside the slab ($k_c^2=k_x^2+\beta^2$) and use Eq. (2.39) with $\alpha=i\beta$, we find that

$$k_c^2=\omega^2\epsilon/c^2, \tag{2.53}$$

i.e., the ω versus k_c dispersion relation in the sinusoidal

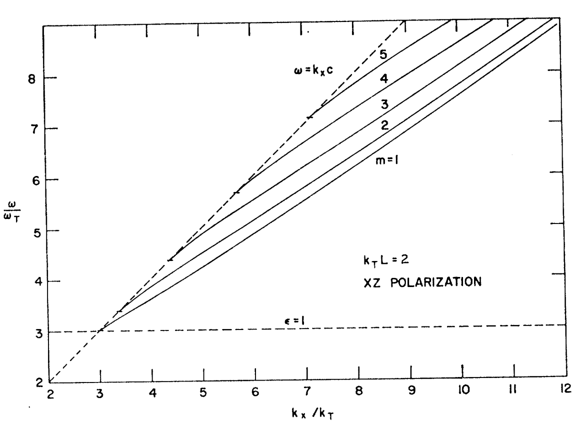

FIG. 6. High-frequency, transverse, optical, xz-polarized modes for a slab of intermediate thickness ($k_TL=z$) with sinusoidal solutions inside the slab.

[5] That all these modes have frequencies below ω_T can be seen as follows: The equations for the surface modes were obtained considering $R_x\neq0$. If $R_x=0$, corresponding to $\omega=\omega_T$, $R_z=4\pi$ and (2.36) becomes $0=\alpha_0^2|_{\omega=\omega_T}-k_x^2$. This equation clearly has no rigorous solutions. However, for $k_x\gg k_T$ it is satisfied approximately, indicating that the mode frequencies approach ω_T in the high k_x limit.

region is identical to that in an infinite crystal, as it must be. From this point of view, the finite size of the crystal makes the allowed values of ω and k_c discrete rather than continuous and gives rise to standing waves rather than traveling waves in the z direction.

If $\beta L \ll 1$, the expressions (2.50) for the polarization for the odd-m modes become $P_x \sim 0$, $P_z \sim$const. This limiting behavior occurs only for the low-frequency $m=1$ mode as $k_x \to 0$ and for the high-frequency $m=1$ mode as $k_x \to 2.998 k_T$.

For all of the sinusoidal modes, just as in the case of the surface modes, the ionic motion is transverse in the sense that $\nabla \cdot \mathbf{P}=0$, but they can interact with conduction electrons because of the finite thickness of the slab.

Suppose that $R_z=0$ or $\omega=\omega_L$. Then, since $R_x=-4\pi$, differentiating Eq. (2.33) yields

$$dP_x/dz = ik_x P_z . \tag{2.54}$$

Assuming

$$P_x = K_3 e^{ik_z z} + K_4 e^{-ik_z z} , \tag{2.55}$$

where k_z is a parameter to be determined, we then have

$$P_z = (k_z/k_x)(K_3 e^{ik_z z} - K_4 e^{-ik_z z}) . \tag{2.56}$$

Putting these expressions into the integral equations (2.33) and (2.34) yields terms with a z dependence of the form $e^{\pm ik_z z}$ or $e^{\pm \alpha_0 z}$. The terms containing $e^{\pm \alpha_0 z}$ cancel, while equating the coefficients of $e^{\pm ik_z z}$ to zero yields once again a pair of linear homogeneous equations for K_3 and K_4. The condition that a solution exists becomes

$$e^{ik_z a} = \mp e^{-ik_z a} . \tag{2.57}$$

Using the upper sign means

$$\cos k_z a = 0 , \quad \text{or} \quad k_z a = m\pi/2 , \quad m=1, 3, 5. \cdots . \tag{2.58}$$

The slab is an integral number of half-wavelengths thick and $K_3=K_4$, so that

$$\begin{aligned} P_x(z) &\propto \cos k_z z , \\ P_z(z) &\propto i(k_z/k_x) \sin k_z z . \end{aligned} \tag{2.59}$$

The lower sign in Eq. (2.57) corresponds to

$$\sin k_z a = 0 , \quad \text{or} \quad k_z a = m\pi/2 , \quad m=2, 4, 6, \cdots . \tag{2.60}$$

The slab is again an integral number of half-wavelengths thick and $K_4=-K_3$, so that

$$\begin{aligned} P_x(z) &\propto i \sin k_z z , \\ P_z(z) &\propto (k_z/k_x) \cos k_z z . \end{aligned} \tag{2.61}$$

Thus, as anticipated, these longitudinal optical modes are identical to those without retardation.

y Direction

The treatment in this case is much like that for the x-z directions and thus will be abbreviated. The condition that the fields remain finite for $|z| \to \infty$ means now that $C_6=C_{17}=0$, from which $C_{15}=C_{16}=0$ and

$$\begin{aligned} C_5 &= -\frac{2\pi i\omega}{\alpha_0 c} \int_{-a}^{a} e^{\alpha_0 z'} P_y dz' , \\ C_{18} &= -\frac{2\pi i\omega}{\alpha_0 c} \int_{-a}^{a} e^{-\alpha_0 z'} P_y dz' . \end{aligned} \tag{2.62}$$

The electric field E_y is given by

$$E_y = \frac{2\pi\omega^2}{\alpha_0^2 c^2} \int_{-a}^{a} G'(z,z') P_y dz' , \tag{2.63}$$

so the equation determining the polarization becomes

$$R_x P_y(z) = \frac{2\pi\omega^2}{\alpha_0^2 c^2} \int_{-a}^{a} G'(z,z') P_y(z') dz' . \tag{2.64}$$

For $R_x \neq 0$, Eq. (2.64) can be converted to the differential equation

$$d^2 P_y/dz^2 = \alpha^2 P_y . \tag{2.65}$$

Writing P_y as

$$P_y = K_5 e^{\alpha z} + K_6 e^{-\alpha z} \tag{2.66}$$

and using this expression in the integral equation (2.64), there results a pair of equations for K_5 and K_6. The condition that these equations have a solution is

$$1 = \frac{\alpha}{\alpha_0} \left(\frac{e^{-\alpha a} \mp e^{\alpha a}}{e^{-\alpha a} \pm e^{\alpha a}} \right) , \tag{2.67}$$

or

$$1 = -(\alpha/\alpha_0) \tanh \alpha a , \tag{2.68}$$

with $K_5=K_6$, and

$$1 = -(\alpha/\alpha_0) \coth \alpha a , \tag{2.69}$$

with $K_5=-K_6$. Clearly Eqs. (2.68) and (2.69) have no solutions for α real. However, if we again make the replacement $\alpha=i\beta$, Eq. (2.68) becomes

$$1 = (\beta/\alpha_0) \tan \beta a , \tag{2.70}$$

while Eq. (2.69) becomes

$$1 = -(\beta/\alpha_0) \cot \beta a . \tag{2.71}$$

Since $R_x=0$ implies $P_y=0$, there are no solutions with $\omega=\omega_L$.

Figure 7 shows the frequencies of these sinusoidal transverse modes as a function of k_x in the region L_1, for a thick slab. The most significant difference between the y-polarized and the xz-polarized modes shown in Fig. 5 is that the dispersion curves leave the line $\omega=k_x c$ much more rapidly for the y-polarized modes, although the starting points are the same. The y-polarized modes in a thin crystal ($k_T L=0.1$) are similar to the xz-polarized modes shown in Fig. 4. However there is again the difference, most significant for the $m=1$ mode, that the

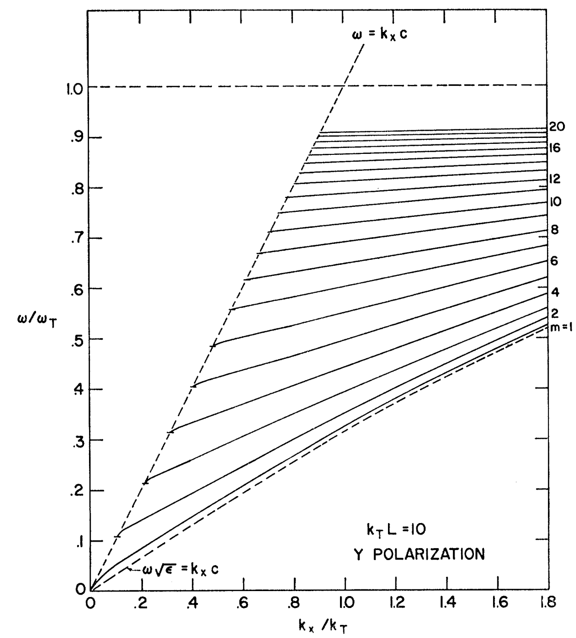

FIG. 7. Low-frequency, transverse, optical, y-polarized modes for a thick slab with sinusoidal solutions inside the slab.

dispersion curves for the y modes do not remain close to the line $\omega = k_x c$.

The z dependence of the polarization P_y for the y modes is similar to that of P_z for the xz modes. Since P_y is parallel to the surface, however, the y modes make no surface contribution to the electron-phonon interaction.

APPENDIX: DETERMINATION OF THE NONRADIATIVE MODES USING THE DIELECTRIC CONSTANT

If the fields are written in the form $\mathbf{E} = \mathbf{E}(z)e^{i(k_x x - \omega t)}$ and $\mathbf{B} = \mathbf{B}(z)e^{i(k_x x - \omega t)}$, Maxwell's equations become

$$-dE_y(z)/dz = (i\omega/c)B_x(z)\,, \tag{A1}$$

$$dE_x(z)/dz - ik_x E_z(z) = (i\omega/c)B_y(z)\,, \tag{A2}$$

$$ik_x E_y(z) = (i\omega/c)B_z(z)\,, \tag{A3}$$

$$-dB_y(z)/dz = -(i\omega/c)\epsilon E_x(z)\,, \tag{A4}$$

$$dB_x(z)/dz - ik_x B_z(z) = -(i\omega/c)\epsilon E_y(z)\,, \tag{A5}$$

$$ik_x B_y(z) = -(i\omega/c)\epsilon E_z(z)\,, \tag{A6}$$

where $\epsilon = 1$ outside the slab and $\epsilon = \epsilon_\infty + (\epsilon_0 - \epsilon_\infty)/(1 - \omega^2/\omega_T^2)$ inside the slab.

First consider longitudinal optical modes with $\epsilon = 0$ and $\omega = \omega_L$. From Eqs. (A4), (A5), (A6), and the continuity of $\mathbf{B}$, it follows that $\mathbf{B} = 0$ everywhere and $\mathbf{E} = 0$ outside the slab. Equation (A3) gives the result $E_y = 0$. Since E_x and ϵE_z are continuous at $z = a$, $E_x(a) = 0$ and $\epsilon E_z(a) = 0 \cdot E_z(a) = 0$ or $E_z(a) \neq 0$. If we try $E_x(z) = A \times \cos k_z z$, Eq. (A2) gives $E_z(z) = iA(k_z/k_x)\sin k_z z$. The condition $E_x(a) = 0$ implies $k_z a = m\pi/2$ with $m = 1, 3, 5, \cdots$. If $E_x(z) = A \sin k_z z$, then $E_z(z) = -iA(k_z/k_x) \times \cos k_z z$, where $k_z a = m\pi/2$, $m = 2, 4, 6, \cdots$. These solutions are identical to those given by Eqs. (2.58) through (2.61).

Now consider transverse optical modes, with $\epsilon \neq 0$. If B_y and E_z are eliminated from Eqs. (A2), (A4), and (A6), the result is

$$dE_z(z)/dz = -ik_x E_x(z)\,, \tag{A7}$$

and

$$d^2E_x(z)/dz^2 - \alpha^2 E_x(z) = 0\,, \tag{A8}$$

where $\alpha^2 = k_x^2 - \omega^2\epsilon/c^2$. The solutions to (A7) and (A8) inside the slab are

$$E_x = e^{\alpha z} \mp e^{-\alpha z}\,,$$
$$E_z = -i(k_x/\alpha)(e^{\alpha z} \pm e^{-\alpha z})\,. \tag{A9}$$

Outside the slab, for $z > a$, we take exponentially decreasing solutions

$$E_x = Ae^{-\alpha_0 z}\,,$$
$$E_z = i(k_x/\alpha_0)Ae^{-\alpha_0 z}\,, \tag{A10}$$

where $\alpha_0^2 = k_x^2 - \omega^2/c^2$. The requirement that E_x and D_z be continuous at $z = a$ yields the condition

$$\epsilon = \frac{\alpha}{\alpha_0}\left(\frac{e^{-\alpha a} \mp e^{\alpha a}}{e^{-\alpha a} \pm e^{\alpha a}}\right), \tag{A11}$$

which is identical to Eq. (2.43). If $\alpha = i\beta$, Eqs. (2.49)–(2.52) follow immediately.

By combining Eqs. (A1), (A3), (A5), we find

$$d^2E_y(z)/dz^2 + \beta^2 E_y(z) = 0\,, \quad |z| < a\,,$$
$$d^2E_y(z)/dz^2 - \alpha_0^2 E_y(z) = 0\,, \quad z > a\,. \tag{A12}$$

Taking solutions of the form $E_y = \sin\beta z$ or $E_y = \cos\beta z$ for $|z| < a$, $E_y = Ae^{-\alpha_0 z}$ for $z > a$, and using the continuity of E_y and B_x at $z = a$, we get the conditions

$$1 = -(\beta/\alpha_0)\cot\beta a \quad \text{for} \quad E_y = \sin\beta z\,,$$
$$1 = (\beta/\alpha_0)\tan\beta a \quad \text{for} \quad E_y = \cos\beta z\,, \tag{A13}$$

as in Eqs. (2.70) and (2.71).